Micro Position Control of a 3-RRR Compliant Mechanism

Merve Acer
Mechanical Engineering
Istanbul Technical University
Istanbul, Turkey
acern@itu.edu.tr

Asif Şabanoviç
Mechatronics Engineering
Sabanci University
Istanbul, Turkey
asif@sabanciuniv.edu

***Abstract*—A 3-RRR compliant mechanism is designed to be used as a micro positioning stage. The stage displacements are analyzed by using structural FEA. However the experimental results for the manufactured mechanism are not compatible with the FEA which are mostly accepted as ideal while designing. A position control using Sliding Mode Control with Disturbance Observer is proposed for the reference tracking of the center of the stage. The motion of the center is measured by using a laser position sensor and the necessary references for the piezoelectric actuators are calculated using the pseudo inverse of the transformation matrix coming from the experimentally determined kinematics of the mechanism. Piezoelectric actuator linear models are used for disturbance rejection. Finally, the position control of the mechanism is succeeded although it has big errors in manufacturing, assembly etc.**

***Index Terms*— 3-RRR mechanism, compliant mechanism, sliding mode control, piezoelectric actuator control, flexure based mechanism, observer.**

I. Introduction

In modern technology positioning parts become very important for micro/nano applications such as cell manipulation, surgery, aerospace, micro fluidics, optical systems, micro machining and micro assembly etc. [1-2]. As a result of these technologies high precision positioning devices with controlled motions at sub-micron is needed. The need of increased accuracy and precision requires the development of design and control methods simple enough that can be used in engineering practice. Traditional rigid body mechanisms start not to provide needed micron range, accuracy and precision. Then high precision mechanisms with flexible joints are designed in which flexible joints transfer necessary motion or force in the mechanism. The desired motion is provided with the deflection of these flexible joints called in the literature as "flexures" and the mechanisms which are composed of flexures instead of rigid joints are called "compliant mechanisms" [3]. These mechanisms have many advantages to be used in high precision applications. The most important advantages are providing high resolution, frictionless, smooth and continuous motion, small displacements up to 0.01 µm, submicron accuracy, being insensitive to temperature changes if they have a symmetrical structure, providing weight reduction, being compact and lastly, being cheaper than the high precision mechanisms that use conventional rigid joints because of the manufacturing costs.

A compliant planar parallel mechanism is decided to be designed in the light of these advantages. The mechanism purpose is to provide micro positioning of necessary parts in x-y axes for the micro manipulation and micro laser machining units in Sabanci University Laboratory. The stage will be used as a fine positioner on the top of a positioner that provides course motion so that smaller pieces can be cut more precisely by using laser source.

Mostly parallel kinematic structures are used for micro positioning stages because of their advantages but parallel kinematic structures have also important disadvantages such as having limited workspace and dexterity, non-linear kinematics, difficult calculation of forward kinematics. However these drawbacks are not problems for flexure based (compliant) mechanisms because the motions are in micro range and due to the small flexure displacements the kinematics can be assumed as linear in the workspace range. The repeatability of these structures is eliminated with flexures because there is no backlash, friction problem in the joints as in rigid mechanisms.

The position tracking control of the compliant micro motion stages is very important because of the high performance requirements in high precision applications. The complexity of modeling of these mechanisms leads to be hard to control its position because of being lack of computing the accurate model. Therefore, a usable method should be defined for controlling the mechanism or the control should eliminate the nonlinearities and uncertainties of the mechanism that is coming from manufacturing and assembly errors.

Parallel kinematic structures have commonly been used while designing compliant positioning stages in the literature. 3-RRR (three revolute joint) kinematic structure is one of the popular kinematic structures [4-10]. The idea of the kinematic structure is to move the triangular stage having 3 revolute joints in 3 chains of links. The end-effector has translation motion along x-y direction and a rotation about the z axis. This type of parallel kinematic structure amplifies the motion of the actuators. The revolute joints were replaced with flexure hinges which were designed according to the desired parallel kinematic performance.

The position tracking of the compliant mechanisms have been studied for high precision applications. A four bar compliant mechanism is designed for micro/nano manipulation and a robust adaptive control methodology is applied by Liaw et al [11]. Another adaptive control has been used by Shieh and Huang to emulate the unwanted behaviors of the mechanism [12]. Chang et al. have designed a x-y-θz piezo micro positioner and used a feedback control to eliminate the hysteresis, nonlinearity and drift of piezoelectric effects [13]. PID control is implemented to a 3-RRR compliant mechanism in [14] using constant Jacobian method presented in [15] Goldfrab has only made the position control simulation of a compliant mechanism by using a sliding mode control [16].

In this paper 3-RRR compliant mechanism is designed. Unpredictable errors coming from manufacturing and assembling errors have been observed when the finite element analysis of the mechanism is compared with the experimental results. The end-effector displacements are extracted experimentally for each actuation direction. Micro position tracking of compliant mechanism is achieved by implementing Sliding Mode Control with Disturbance Observer (DOB) using linear piezoelectric actuator (PEA) models to get rid of the uncertainties in the mechanism.

In Sec. II 3-RRR compliant mechanism is introduced. The FEA, the experimental setup, the comparison results of experimental results and FEA results are presented in Sec. III. The workspace of the mechanism is also shown in Sec. III. The control methodology is explained in Sec IV. The position control results are shown and discussed in Sec V. Finally a conclusion has been made in Sec. VI.

II. 3-RRR Compliant Mechanism

RRR compliant mechanism is designed by using circular notch flexure hinges as shown in Fig. 1. As mentioned earlier circular notch hinges are picked as revolute joints because they relief the undesired stress on the beams and they can keep their position of rotation center stable so they are less sensitive to parasitic motions than the beam shaped flexures. The stage is actuated by driving a kind of lever mechanisms with piezoelectric actuators. The end-effector of the mechanism is a triangular stage which connects the three RRR links and has motion x-y directions and a rotation about z-axis.

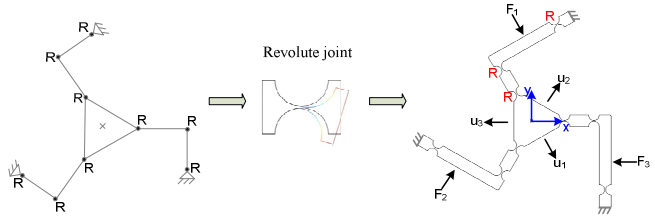

Fig. 1. 3-RRR compliant stage with circular flexure hinges.

Although the mechanism has 3 DOF (x-y and rotation about z axis) we will deal only with the x-y motion of the stage. As mentioned earlier we will use the redundancy of the mechanism to increase the range of the stage and dexterity. The mechanism can be driven as illustrated in Fig. 2. The RRR links are actuated by forces F_1, F_2 and F_3 to create the displacements of u_1, u_2 and u_3 respectively. By the combination of the "u" displacements desired x-y motion of the triangular stage can be generated.

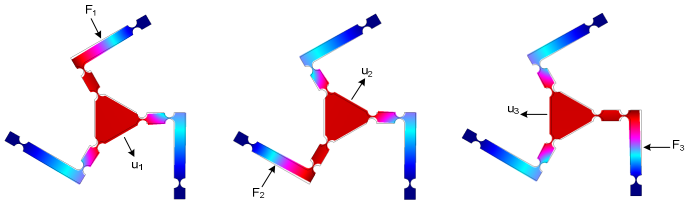

Fig. 2. 3-RRR compliant mechanism displacements.

A hexagonal case is also designed outside the mechanisms range so that it can be fixed to the experimental setup properly. The mechanism shown in Fig. 3 is manufactured by using wire electrical discharge machining (Wire EDM) technique by using Aluminum 7075. The shortest thickness of the flexure is 0.8 mm and the overall thickness of the mechanism in z axis is 10 mm.

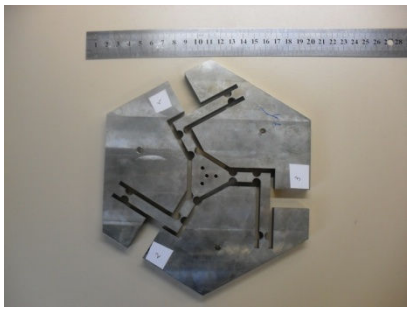

Fig. 3. 3-RRR compliant mechanism.

III. FEA Analysis and Experimental Results of The Compliant Mechanism

A. FEA Analysis

Finite element analysis software called COMSOL is used for analyzing the displacement-force characteristic of 3-RRR compliant mechanism. Plane stress elements which have 2 degrees of freedom have been used for meshing. 2D triangular plane stress elements are preferred for predicting the stiffness values of a flexure hinge instead of plane strain elements because Schotborgh [17] has proved that plain stress elements make safer estimations. Mapped meshing technique is used to control the distribution of number of elements. The number of elements is increased on the boundaries which are near the hinge until the results are converged to the same number.

2D triangular plane stress elements are used for the meshing of the 3-RRR compliant mechanism and the number of elements is set as 7844 elements and number of degrees of freedom is 33574 after much iteration to find a convergence.

B. The Experimental Setup

The setup shown in Fig. 4 is composed of the mechanism, three piezoelectric actuators, a base table, three sliding stages with micrometers, a laser position sensor and a middle base. The piezoelectric motor used is piezomechanik's PST 150/5/40

VS10 type which has max stroke 55 µm for semibipolar -30 V/ +150 V activation and 40 µm stroke for unipolar 0V/+150V activation. Piezomechanik's analog amplifier SVR 150/3 is also used for actuating the piezos. PI's P-853 piezoelectric micrometer drives with sliding stages are put in x and y directions according to the links of the mechanisms so that we can manually preload the mechanism and drive the prismatic joints correctly. The measurement system is shown in Fig. 5 which is composed of a 4mm x 4mm dual axis position sensing diode on a PCB (DL 16-7PCBA3) placed on the triangular effector's center and a assembled laser source on the top of the position sensing diode.

The piezo amplifiers inputs and the laser dual axis position outputs are connected to dSPACE 1103 controller board through DACs and ADCs. Control Desktop is used for CPU calculations for the controller.

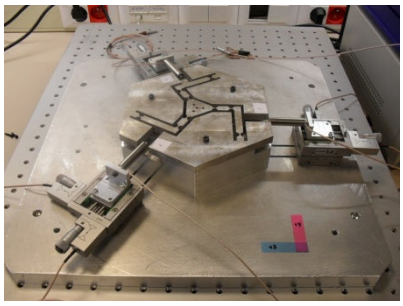

Fig. 4. Assembling of manufactured parts of experimental setup

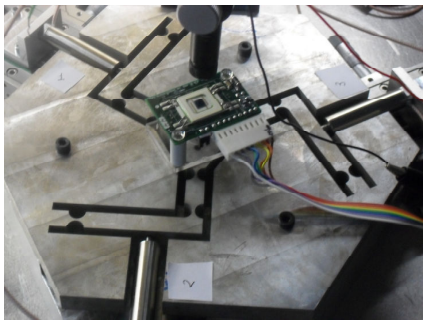

Fig. 5. The dual position sensor and the laser source.

C. The Results

The workspace of 3-RRR compliant mechanism is determined by setting 150 V which provides the maximum strokes (40 µm) to the piezoelectric actuators. The actuations are done individually and by the combinations with each other. The maximum displacement results of the center of the stage which shows the workspace of the stage is drawn in Fig. 6 which presents a hexagonal workspace. The shape of the hexagonal is distorted so we can say that we have errors due to manufacturing and assembling the mechanism.

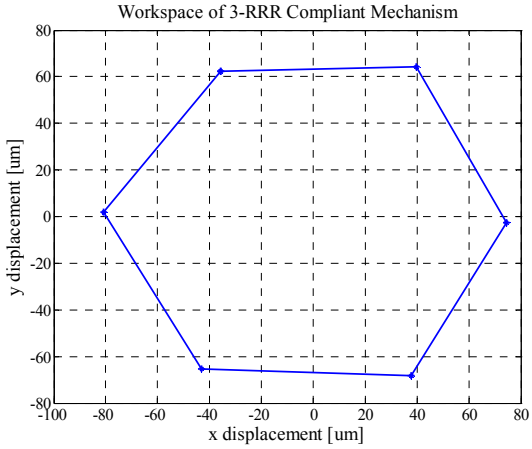

Fig. 6. Workspace of 3-RRR compliant mechanism.

The experimental results of the displacement of the end effector is compared with the FEA results in order to see how much we are far from the ideal case of the mechanism. 12, 24, 36, 48 and 60 µm input displacements are given to each of the piezoelectric actuators, respectively when all piezoelectric actuators are assembled to the mechanism, and they are all preloaded ready to drive the link that they are connected to.

The results, which present the x-y displacements for each u_{in1}, u_{in2} and u_{in3} input displacements, are shown in Fig. 7.

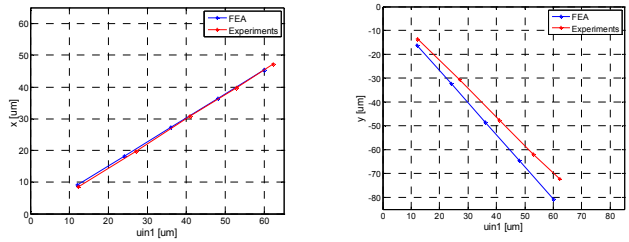

(a) Results for u_{in1}

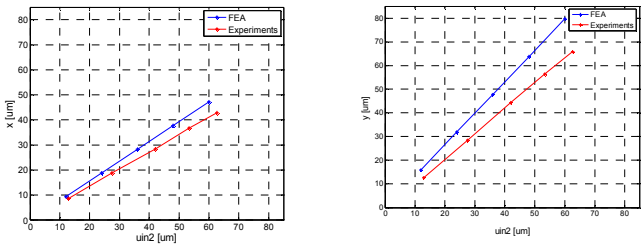

(b) Results for u_{in2}

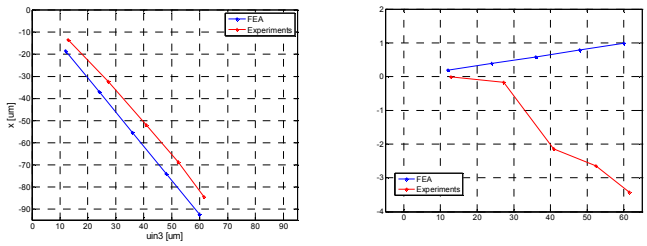

(c) Results for u_{in3}

Fig. 7. Comparison of experimental and FEA results or 3-RRR compliant mechanism.

The % errors of x-y axes when compared to FEA for each input are presented in Table 1. There is a large y motion in the manufactured mechanism, whereas in FEA results the y motion is very small when only piezo 3 is actuated. The resulting motions in the other directions have errors up to 21% when looking at the results. Thus, we need to eliminate these errors by control methods.

TABLE I. % ERRORS COMPARED TO FEA FOR 3-RRR

uin_1		uin_2		uin_3	
% error for x	% error for y	% error for x	% error for y	% error for x	% error for y
-0.088	13.75	12.87	20.95	10.86	4.39e2

D. Kinematics of The Mechanism

T. S Smith says in his work that no matter how crude the machining the displacement characteristics of compliant mechanisms will remain linear, the axis of the motion will change [18]. We have experimentally determined the direction of the displacement vectors u_1, u_2 and u_3 to have the kinematics of the mechanism shown in Fig. 5. After calibration of laser position sensor, we have applied respectively 30, 60, 90, 120 and 150 Volts to the piezoelectric actuators when all the piezoelectric actuators are assembled to the mechanism and preloaded before starting actuation. The results of the experiments are shown in Fig. 6. The transformation matrix **A** which relates the motions u_1, u_2 and u_3 to x-y motion of the end-effector can be written as in Eqn. 1:

The angles of the direction of the u vectors are found as θ_1=26º, θ_2=25º and θ_3=1.5º.

$$\begin{bmatrix} x \\ y \end{bmatrix} = \underbrace{\begin{bmatrix} \sin(\theta_1) & \cos(\theta_2) & -\cos(\theta_3) \\ -\cos(\theta_1) & \sin(\theta_2) & -\sin(\theta_3) \end{bmatrix}}_{\boldsymbol{A}} \cdot \begin{bmatrix} u_1 \\ u_2 \\ u_3 \end{bmatrix} \quad (1)$$

IV. POSITION CONTROL METHODOLOGY

A. Piezoelectric Actuator Model

Piezoelectric actuators electromechanical lumped model can be defined by the equations (2)-(7) [19]. The model is shown in Fig. 8 where v is the total voltage across the actuator, v_p is the piezoelectric voltage and v_h is the hysteresis voltage. T is the electromechanical transformation ratio that connects electrical part and mechanical part of the model. q is the total charge in the actuator, q_p is the charge transduced due to mechanical motion, H is the hysteresis function that depends on q, F_p is the force of the piezoelectric effect and F_{ext} is the external force on the actuator. According to equation (7) u is the displacement, m_p, c_p and k_p are respectively the equivalent mass, damping and stiffness of the piezoelectric actuator. F_c is the control force and F_{dis} is the disturbance force.

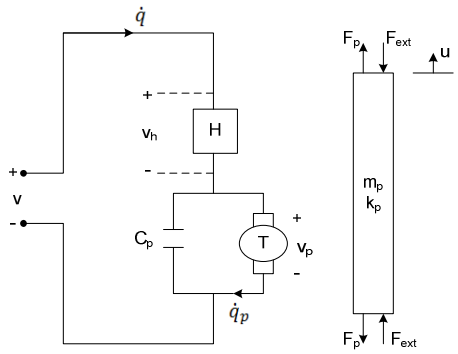

Fig. 8. Piezoelectric actuator model [19].

$$v_p = v - v_h \quad (2)$$
$$v_h = H(q) \quad (3)$$
$$q = Cv_p + q_p \quad (4)$$
$$q_p = Tu \quad (5)$$
$$F_p = Tv_p \quad (6)$$
$$m_p\ddot{u} + c_p\dot{u} + k_p u = \underbrace{Tv}_{F_c} - \underbrace{Tv_h - F_{ext}}_{F_{dis}} \quad (7)$$

B. Disturbance Observer

We are able to eliminate disturbances by modeling an observer so a linear model is defined by using nominal parameters of actuator as in equation (10). The displacement u for every piezoelectric actuator can be measurable by using laser position sensor and inverse of the transformation matrix. The supply voltage is also measurable. The linear model of the piezoelectric actuator is:

$$m_n\ddot{u} + c_n\dot{u} + k_n u = T_n v - F_d \quad (10)$$

We can define F_d as hysteresis force, external force and the uncertainties of the plant parameters which are Δm, Δc, Δk and ΔT. These parameters are assumed as bounded and continuous.

$$F_d = T_n v_h + F_{ext} + \Delta T(v_h - v) + \Delta m\ddot{u} + \Delta c\dot{u} + \Delta k u \quad (11)$$

The observer can be designed as a position tracking system in which F_d is replaced with an observer control $T_n v_{obsc}$ because u and v_{in} can be measured and the observer transfer function is written as following equation.

$$m_n\ddot{\hat{u}} + c_n\dot{\hat{u}} + k_n\hat{u} = T_n v_{in} - T_n v_{obsc} \quad (12)$$

$\hat{u}$ is the estimated position, v_{in} is the plant control input, v_{obsc} is the observer control input. When $\hat{u}$ tracks u, F_d equals to $T_n v_{obsc}$. A sliding manifold is selected for that purpose which is $\sigma = \dot{u} - \dot{\hat{u}} + C_{obs}(u - \hat{u})$. The Lyapunov function is taken as $v_L = {\sigma^2}/{2}$ which is positive definite and the derivative of Lyapunov function is taken as $-D_{obs}\sigma^2$ which is negative definite. We will get equation (13) by equating the above results and simplifying:

$$L = \sigma\dot{\sigma} = -D_{obs}\sigma^2 \Rightarrow \dot{\sigma} + D_{obs}\sigma = 0 \quad (13)$$

If we insert sliding mode manifold into the equation (13):

$$\left(\ddot{u} - \ddot{\hat{u}}\right) + (C_{obs} + D_{obs})\left(\dot{u} - \dot{\hat{u}}\right) + C_{obs}D_{obs}(u - \hat{u}) = 0 \quad (14)$$

When we subtract the equations (12) from (11) and insert the result into the above equation (14) we can find the equivalent control v_{eqc} which keeps system motion in manifold $\sigma + \dot{D}\sigma = 0$.

$$v_{eqc} = \frac{1}{T_n}\{F_d + [c_n - m_n(C_{obs} + D_{obs})](\dot{u} - \dot{\hat{u}})[k_n - m_n C_{obs} D_{obs}](u - \hat{u})\} \quad (15)$$

Equation (15) tells us that when $\sigma \to 0$ then $u \to 0$and $T_n v_{eqc} \to F_d$. For the implementations discrete form of sliding mode control is used as:

$$v_{(k)} = v_{(k-1)} + K_{uobs}\left(D_{obs}\sigma_{(k)} + \frac{\sigma_{(k)} - \sigma_{(k-1)}}{dT}\right) \quad (16)$$

K_{uobs} is a design parameter that optimizes the controller and dT is the sampling interval for discrete time control. The system and the observer can be summarized as in equations (17-19):

$$m_n\ddot{u} + c_n\dot{u} + k_n u = T_n v_{in} - F_d \quad (17)$$

$$m_n\ddot{\hat{u}} + c_n\dot{\hat{u}} + k_n\hat{u} = T_n v_{in} - T_n v_{obsc} \quad (18)$$

$$v_{in} = v_c + \frac{\alpha}{T_n} v_{obsc} \quad (19)$$

C. Sliding Mode Position Control

The sliding manifold is selected to be as in equation (20) and when the sliding manifold is reached the closed loop control showed in equation (21) and the system is described by equation (22).

$$\sigma_x = (\dot{u}_{ref} - \dot{u}) + C_x(u_{ref} - u) \quad (20)$$

$$v_{(k)} = v_{(k-1)} + K_{ux}\left(D_x\sigma_{x(k)} + \frac{\sigma_{x(k)} - \sigma_{x(k-1)}}{dT}\right) \quad (21)$$

$$(\ddot{u}_{ref} - \ddot{u}) + (C_x + D_x)(\dot{u}_{ref} - \dot{u}) + C_x D_x(u_{ref} - u) = 0 \quad (22)$$

Figure 9 presents our proposed control method which is the combination of the sliding mode position control with the disturbance observer based on sliding mode control for each piezoelectric actuator. The *i* subscript defines the number of piezoelectric actuator and its actuation direction.

The conversion between the actuation positions u_i and the center positions (x, y) are carried out like explained in eqn. (23).

$$\boldsymbol{u_i} = \boldsymbol{A}^{\dagger}[x\ y]^T \quad (23)$$

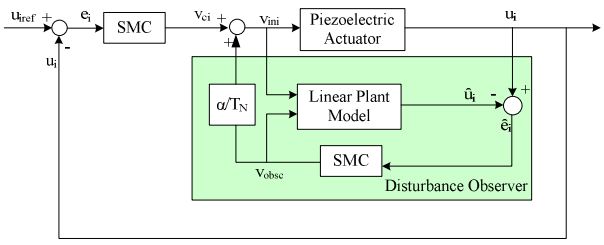

Fig. 9. Closed loop control block diagram

V. Results

The position control method is implemented for each actuation direction by coding the calculations in C according to the control scheme shown in Fig. 9. A circular trajectory has given to the center of the mechanism with the diameter of 30 µm. So the references in x and y axes are set as:

$$x_{ref} = 15 + 15\sin(0.2\pi t) \quad (24)$$

$$y_{ref} = 15 + 15\cos(0.2\pi t) \quad (25)$$

The pseudo inverse of transformation matrix **A** as in eqn. (1) is used for calculating the necessary position references for the u_{ref1}, u_{ref2} and u_{ref3}. The control input voltages is saturated between 0V to 150V to use the bipolar actuation property of the piezoelectric actuators. All calculations in C are done in metric unit. The sampling time for computing is 100 µsec which is necessary time for the calculations in dSPACE. The nominal parameters of used PSt 150/5/40 VS10 Piezoelectric actuators are shown in Table 2.

TABLE II. Nominal parameters of PST 150/5/40 VS10 Piezoelectric Actuator

Parameter	Value
m_n	$6.16 \cdot 10^{-4}$ kg
c_n	1027.5 Ns/m
k_n	$12 \cdot 10^{6}$ N/m
T	3.1 N/V
α	0.05

Figure 10 shows how the center of the stage tracks the reference which is a circle having 30 µm of diameter. The errors in x direction shown in fig. 10 is between -0.35 µm and -0.75 µm whereas the errors in y direction shown in fig. 11 is between 0.1 µm and -0.28 µm. The DOB rejects the unpredictable disturbances and SMC succeeds to track the reference position. The position control of the mechanism can be acceptable when the unpredictable errors are up to %21 when compared to FEA which is accepted as the ideal case of the mechanism.

It can be seen from the figs. 11 and 12 that the errors in x and y direction have jumps. This is because the voltage input to the piezoelectric actuators is saturated between 0 V-150 V not allowing negative values of voltages and the piezoelectric actuators are not fixed to the mechanism; they are just preloaded before actuation and can't pull back the links. This situation can be fixed by having a better observer and tuning the parameters.

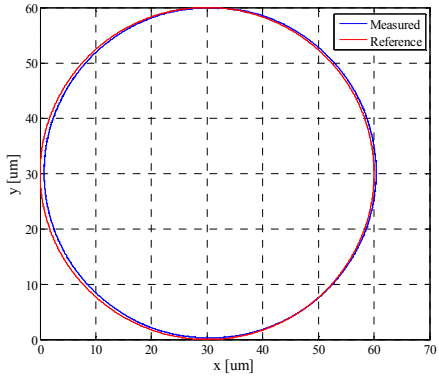

Fig. 10. The measured x-y motion of the center of the stage.

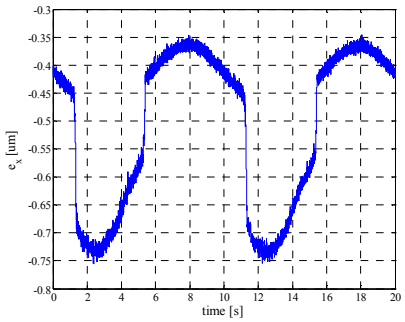

Fig. 11. Error in x direction.

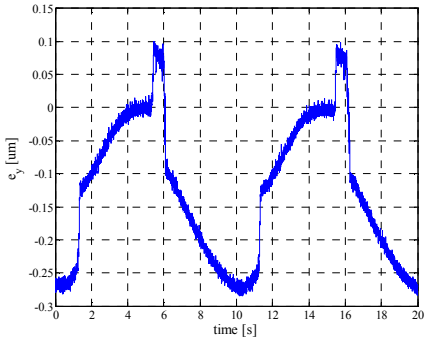

Fig. 12. Error in y direction.

VI. CONCLUSION

A compliant mechanism to be used as a micro positioned for micro system applications in the laboratory is designed based on 3-RRR kinematic structure. FEA of the mechanism for the center displacement is carried out by using COMSOL. The analysis results are compared with the manufactured mechanism experimental results and it's seen that there are up to %21 errors. These errors are mainly due to rough manufacturing and assembly.

The system is treated as a 3 single input single output system for the control purposes because the kinematic structure decouples the stiffness between actuators. So, a transformation matrix is found between the actuation directions and x-y axes. Then a control scheme based on SMC and DOB is implemented for each piezoelectric actuator. Linear models of the piezoelectric actuators are used as nominal models to get rid of the uncertainties and errors in the mechanism. Finally, the results show us that we are able to control a compliant mechanism in micro level which has erroneous motion compared to the ideal case by using SMC with DOB. For the future work the control can be tuned more precisely or another model can be used for disturbance rejection to improve the reference tracking.

REFERENCES

[1] A. H. Slocum, Precision Machine Design. New Jersey, USA: Prentice Hall, 1992.

[2] D.G.Chetwynd S.T. Smith, Foundations of Ultraprecision Mechanism Design. North Carolina, USA: CRC Press, 1994.

[3] Nicolae Lobontiu, Compliant Mechanisms: Design of Flexure Hinges.: CRC Press, 2003.

[4] B. Shirinzadeh, D. Zhang Y. Tian, "Design and dynamics of a 3-DOF flexure-based parallel mechanism for micro/nano manipulation," Microelectronic Engineering, vol. 87, no. 2, pp. 230–241, February 2010.

[5] Daniel C. Handley, Yuen Kuan Yong, Craig Eales Tien-Fu Lu, "A three-DOF compliant micromotion stage with flexure hinges," Industrial Robot: An International Journal, vol. 31, no. 4, pp. 355 - 361, 2004.

[6] W. Szyszkowski, W.J. Zhang B. Zettl, "Accurate low DOF modeling of a planar compliant mechanism with flexure hinges: the equivalent beam methodology," Precision Engineering, vol. 29, no. 2, pp. 237–245, April 2005.

[7] J. Zou, L. G. Watson, W. Zhao, G. H. Zong, S. S. Bi W. J. Zhang1, "The Constant-Jacobian Method for Kinematics of a Three-DOF Planar Micro-Motion Stage," Journal of Robotic Systems, vol. 19, no. 2, pp. 63-72, February 2002.

[8] Tien-Fu Lu, Daniel C. Handley Yuen Kuan Yong, "Loop Closure Theory in Deriving Linear and Simple Kinematic Model for a 3 DOF Parallel Micromanipulator," , Perth, 2003.

[9] Tien-Fu Lu, J. Minase Y. K. Yong, "Trajectory Following with a three-DOF Micro-motion Stage," ,Auckland, 2006.

[10] D.C. Handley, Yuen Kuan Yong Tien-Fu Lu, "Position Control of a 3 DOF Compliant Micro Motion Stage," , 2004.

[11] H. C.Liaw, B Shirinzadeh, J. Smith, "Robust motion tracking control of piezo-driven flexure-based four-bar mechanism for micro/nano manipulation",2007.

[12] Shieh, H.J.; Huang, P.K.; , "Adaptive Tracking Control of a Piezoelectric Micropositioner," Industrial Electronics and Applications, 2006 1ST IEEE Conference on , vol., no., pp.1-5, 24-26, May 2006

[13] S.H. Chang, C.K. Tseng and H.C. Chien, An ultra-precision XYθz piezo-micropositioner. Part II. Experiment and performance. IEEE Transactions on Ultrasonics, Ferroelectrics, and Frequency Control, 46 4, pp. 906–912, 1999.

[14] Tien-Fu Lu, Daniel C. Handley, Yuen Kuan Yong, Craig Eales, "A three-DOF compliant micromotion stage with flexure hinges", Industrial Robot: An International Journal, Vol. 31 Iss: 4, pp.355 – 36, 2004.

[15] Zhang W. J., Zou J., Watson G., Zhao W., Zong G. and Bi S., "Constant-Jacobian method for kinematics of a 3-DOF planar micro-motion stage", Journal of Robotic Systems, Vol. 19, No 2, pp. 63-79, 2002.

[16] Fite, K.; Goldfarb, M., "Position control of a compliant mechanism based micromanipulator," Robotics and Automation, 1999. Proceedings. 1999 IEEE International Conference on , vol.3, no., pp.2122-2127 vol.3, 1999.

[17] F. G. M. Kokkeler, H. Tragter, F. J. A. M. van Houten W. O. Schotborgh, "Dimensionless design graphs for flexure elements and a comparison between three flexure elements," *Precision Engineering*,vol.29,pp.41-47,2005.

[18] Smith, S. T.; Chetwynd, D. G.; Bowen, D. K., "Design and assessment of monolithic high precision translation mechanisms", Journal of Physics E: Scientific Instruments, Volume 20, Issue 8, pp. 977-983, 1987.

[19] Michael Goldfrab and Nikola Celanovic, "Modeling Piezoelectric Stack Actuators for Control of Micromanipulation", IEEE Cont. Ss. Mag., Vol 17, pp. 69-79, 1997.